MICHIGAN STATE UNIVERSITY

CYCLOTRON LABORATORY

LIQUID-GAS PHASE INSTABILITIES IN NUCLEAR SYSTEMS

M.W. CURTIN, H. TOKI, and D.K. SCOTT

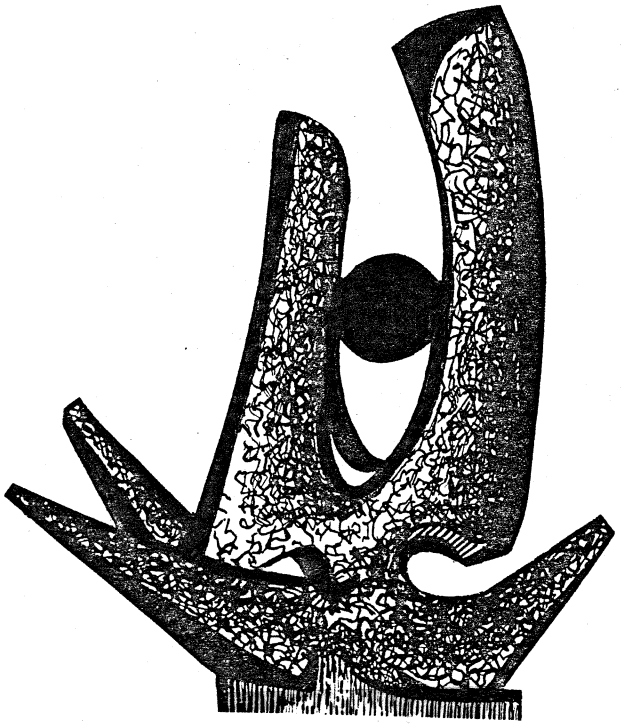

MAY 1982

MSUCL-373

MSUCL-373
May 1982

LIQUID-GAS PHASE INSTABILITIES IN NUCLEAR SYSTEMS

M.W. Curtin, H. Toki, and D.K. Scott

National Superconducting Cyclotron Laboratory
Michigan State University
East Lansing, Michigan 48824, USA

Abstract

The conventional approach to composite fragment production in heavy ion collisions from a single gaseous phase may require modification at temperatures below 20 MeV due to the onset of a liquid-gas phase instability. Clusters heavier than the α-particle are necessary for an unambiguous experimental signature.

PAC NOS. 25.70.Fg, 05.70.Jk, 24.90.+d

In high energy nuclear collisions, a localized zone of participant nucleons can be created at excitation energies greater than the binding energy of the nucleons. The disassembly of the hot transient system into many different final channels is a problem of current interest.[1] Thermodynamic models have been developed to account for the emission of light composite fragments by treating the participant zone as a single gaseous phase in thermal and chemical equilibrium. However, under certain combinations of density and temperature the system may develop an instability toward division into liquid and gas phases which could influence the production of composite fragments. In this paper we discuss the conditions for this instability to develop and we suggest how this effect might be observed experimentally.

To derive the condition for a liquid-gas instability, we start from the relation[2]

$$\rho = \frac{4}{(2\pi)^3} \int d^3k \, [1 + \exp(\frac{k^2}{2m} - \mu)/T]^{-1}$$

from which the chemical potential, μ, is determined as a function of the density ρ and the temperature T. The thermal contribution to the internal energy is given by

$$\frac{E_T}{V} = \frac{4}{(2\pi)^3} \int d^3k \, \frac{k^2}{2m} \, [1 + \exp(\frac{k^2}{2m} - \mu)/T]^{-1}$$

using the calculated values of μ. The pressure due to the thermal motion is then $2E_T/3V$ corresponding to a zero point pressure of $\frac{2}{5}\,\epsilon_F(\rho)$ where ϵ_F is the Fermi Energy. The total pressure is the sum of the thermal pressure and the pressure, P_V due to the interaction among the constituents of the system. To derive P_V we express the energy per nucleon in the form[3] obtained from a Skyrme type interaction

$$\frac{E_V}{A} = -A\rho + B\rho^{\sigma+1}$$

where A and B are constants determined by the constraint $E/A = -16$ MeV (for nuclear matter) when $\rho = \rho_o$ together with the further condition for stability of normal density nuclear matter, $\partial(E/A)/\partial\rho = 0$.

Solving for A and B with $\epsilon_F\ (\rho=\rho_o) = 38$ MeV and $\sigma = 2/3$ we find $A\rho_o = 74.2$ MeV and $B\rho_o^{5/3} = 35.4$ MeV. In general A and B have some temperature dependence but here we assume that the thermal and interaction energies and pressures are separable. The pressure due to the interaction (at T=0) is $\rho^2\ \partial(E/A)/\partial\rho$, resulting in

$$\frac{P_V}{\rho} = -A\rho + \frac{5}{3}B\rho^{5/3}$$

The total pressure as a function of density for constant temperature is plotted in fig. 1, which shows that the equation of state has the form typical of a Van der Waal's system with liquid and gaseous phases. For the unphysical region

(shown only for T=15 MeV) where the slope is negative (implying a negative incompressibility) a Maxwellian construction is employed, along which the liquid and gas phases coexist. The region of coexistence is indicated in the figure. The range of densities compatible with coexistence becomes smaller as the temperature increases until the apex of the coexistence region coincides with the inflection point of the critical temperature curve. At this critical temperature $T_c \simeq 20$ MeV the co-existence of liquid and gas phases is possible only at $\rho_c \simeq 0.07\,\mathrm{fm}^{-3}$ and only a gaseous phase exists for all higher temperatures. Our results are in good agreement with recent calculations.[4]

Our choice of parameters leads to an incompressibility of 310 MeV.[5] Current estimates from nuclear monopole excitations indicate that the incompressibility is $\simeq 210$ MeV.[6] In our calculation we let $E/A = -16$ MeV (ignoring surface effects) and $\sigma = 2/3$ in the Skyrme interaction. The thermodynamic treatment implies a large system and hence $E/A = -16$ MeV is fixed. If σ is allowed to change to reproduce K=210 MeV, a critical temperature of 17 MeV is predicted.

In order to discuss the observable consequences of the phase instability at T_c, several points must be considered. First, the relevance of the isotherms in fig. 1 to the actual evolution of the disassembling nuclear system must be considered. According to cascade model calculations[7] at incident energies $\lesssim$250 MeV/u the temperature does not vary rapidly as a function

of time and consequently the time evolution of the system may be considered isothermic for the temperature in the critical region of 20 MeV, corresponding to incident energies of ~100 MeV/u. In contrast to the cascade model, hydrodynamical calculations indicate that entropy, as opposed to temperature, may remain constant during expansion. Recent hydrodynamical calculations[8] indicate that constant temperature in the critical range is, however, a plausible assumption. In this paper we assume that a constant temperature is appropriate to the disassembly process.

Finally, we must note that during the disassembly phase of the hot region, the density decreases until the thermal freeze out density (ρ_f) is reached. This density is roughly defined when the mean free path becomes commensurate with the physical size of the hot region. Collisions cease at ρ_f and the fragments travel undisturbed to the detectors aside from final state interactions.[9] To observe both liquid and gas phases at a given temperature the Maxwellian construction must encompass ρ_f. If ρ_f is large then the system will be in the liquid phase at freeze out, whereas if ρ_f is small only the gas phase will exist signifying that the system has traversed the coexistence portion of the isotherm and the liquid phase no longer exists.

In the event that $\rho_f < \rho_c$ the system will enter the gas phase prior to freeze out leading to an erroneous interpretation of T' (see fig. 1) as the critical temperature T_c. Further inspection of fig. 1 indicates that for $\rho_f \geq \rho_c$ the temperature T_c will be correctly identified. The smallest value of

ρ_f quoted in ref. 10 is 0.4 ρ_o ($\pm$ 30%) allowing us to set a lower limit on ρ_f of 0.05 fm^{-3}. As illustrated in fig. 1 the coexistence boundary intersects this minimal ρ_f on the T ≈19 MeV isotherm, leading to an error in the determination of the critical temperature of 1 MeV. As we shall see below it is difficult to extract experimental temperatures with greater accuracy.

In a recent paper[11] the trends of emitted light particles (p,d,t, ^{3}He, α) were studied. For each reaction a component in the energy spectra was attributed to emission from a localized participant source of velocity intermediate between those of projectile and target and the associated temperatures were deduced. The integrated cross-sections from the source for each particle are shown in fig. 2. The curves are labeled by the incident energy, projectile and target on the left. Temperatures are labeled on the right. In each case a range of temperatures is indicated accommodating the limits for fitting spectra of different emitted particles.

At high incident energies, corresponding to high temperatures, the yield falls off monotonically as a function of particle mass. This behavior is expected for emission of clusters from a high temperature single gaseous phase where the composite production cross section can be related to a power of the nucleon cross section. This result is common to both the coalescence and thermal models. In the region of E_{inc} ≈100 MeV/u corresponding to T ≈20 MeV, the distribution flattens and

at still lower temperatures the trend reverses so that the alpha particle yield exceeds that of lighter particles. While it is tempting to attribute this enhanced cluster formation at temperatures below 20 MeV to the onset of the liquid-gas instability we have discussed, it is necessary first to study the consequences of the large alpha binding energy in the gas model.

From the standpoint of internal energy it is very favorable to form an alpha since the binding energy per nucleon (at $\rho = \rho_o$ and $T = 0$) is 7.1 MeV. Since the entropy steadily decreases with increasing fragment mass, the formation of a carbon nucleus is less favored than an alpha particle although the binding energies per nucleon are comparable. The binding energy per nucleon of the alpha far exceeds any of the nearest neighbors thus making it a very favorable structure . Bearing this in mind, we construct a gas composed of alphas and nucleons. The partition function for alphas and nucleons is

$$Z = \frac{1}{N_n!}\,(4\, q_n\, V_n)^{N_n} \cdot \frac{1}{N_\alpha!}\,(q_\alpha\, V_\alpha\, e^{B/T})^{N_\alpha}$$

where $q_i = (M_i T/2\pi\hbar^2)^{3/2}$, the quantum concentrations for nucleons and alphas. The free energy is defined as $F = -T \ln Z$. Furthermore, we require $\partial F/\partial N_\alpha = 0$. To account for the hard core of the alpha we replace V_α by V'_α where

$V'_\alpha = V_\alpha - N_\alpha v_\alpha$ and the excluded volume $v_\alpha \approx (4\pi/3)\,(2)^3$ fm^3.

The number of nucleons participating in the interaction region was chosen to be 40 commensurate with the geometry of the participant zone and with experimental determinations (see ref. 10 and references therein). The ratios N_d/N_p and $(N_t + N_{^3He})/N_p$ are assumed constant and equal to 1/3 and 1/10 respectively.[12] The freeze out density was fixed at 0.05 fm^{-3}. (However, the results are not significantly different for $\rho_f = 0.08$ fm^{-3}.) The results of the calculation in fig. 3 reproduce the trends of the experimental data and reinforce the idea that light particle emission has a thermal origin. It would be difficult, for example, to explain these results with a final state coalescence model. The influence of a liquid-gas phase instability may be more clearly discernable in the cross sections for heavier clusters (A>4), which are likely to be enhanced at the onset of the liquid phase but which are strongly disfavored in the simple gas model. In this context we note the recent observation in relativistic proton induced spallation of heavy targets: the yield for fragments of mass A is of the form $Y(A) \propto A^{-x}$ where $2 \leq x \leq 3$.[13] Such a power law distribution is expected of systems at the critical point for condensing to the liquid phase.[14]

In this paper we have shown that a liquid-gas phase instability may develop in nuclear systems when $T \lesssim 20$ MeV. At higher temperatures existing experimental data on light composite fragment production appear consistent with emission

from a gaseous phase. The observed enhancement of alpha particles at lower temperatures cannot, at present, be unambiguously attributed to the formation of clusters expected at the onset of the liquid phase, since the large binding energy per nucleon of the alpha particle also favors its production in a single phase gas model. The influence of a liquid phase transition might be more readily observable in the production of heavier clusters which should be strongly inhibited in the non-interacting gas model.

It is clearly of interest to incorporate the effects discussed here into more detailed dynamical models, particularly in the hydrodynamical model which can deal with the equation of state at low density. The observable consequences of a phase transition may have implications for transitions that are conjectured to occur at greater than normal nuclear density.

We wish to thank G.F. Bertsch, P.J. Siemens and W. Friedman for informative discussions as well as the authors of ref. 11 for permission to use unpublished data. This material is based upon work supported by the National Science Foundation under Grant No. PHY 80-17605, and supported by U.S. DOE Contract DE-AC02-80ER10579.

References

1. J. Randrup and S.E. Koonin, Nucl. Phys. A356, 233 (1981); G. Fai and J. Randrup, Lawrence Berkeley Laboratory Report No. LBL 13357 (1981)
2. C. Kittel and H. Kroemer, Thermal Physics (W.H. Freeman and Co., San Francisco, 1980)
3. L. Zamick, Phys. Lett. 45B, 313 (1973)
4. B. Friedman and V.R. Pandharipande, Nucl. Phys. A361, 502 (1981); G. Ropke, L. Munchow and H. Schulz, Preprint, 1982
5. M.A. Preston and R.K. Bhaduri, Structure of the Nucleus (Addison-Wesley, Massachusetts, 1975)
6. F. Serr, G. Bertsch and J.P. Blaizot, Phys. Rev. 22, 922 (1980)
7. K.K. Gudima and V.D. Toneev, Joint Institute for Nuclear Research Preprint E2-12621 Dubna, 1979
8. H. Stöcker, Lawrence Berkeley Laboratory Preprint LBL - 12302 (1981)
9. A. Mekjian and D. Gupta, Phys. Rep. 72C, 133 (1981)
10. M.C. Lemaire et al, Phys. Lett. 85B, 38 (1979)
11. G.D. Westfall et al, Michigan State University Preprint MSUCL-365 (1982)
12. S. Nagamiya et al, Phys. Rev. C 24, 971 (1981)
13. R.W. Minich et al, Purdue University Preprint, 1982
14. M.E. Fisher, Physics 3, 255 (1967)

Figure Captions

Fig. 1. Pressure versus density for fixed temperature is plotted. Solid curves indicate paths traversed by a system with fixed T. Liquid, gas and coexistence (hatched) regions are indicated. The significance of ρ_f, ρ_c and T′ are discussed in the text.

Fig. 2. Cross-sections for different fragment masses are plotted for a range of incident energies (shown on the left) and equivalent temperatures (right). Error bars are indicated for highest (X) and lowest (●) incident energies.

Fig. 3. The α-particle yield predicted by minimizing the free energy, keeping the ratios N_d/N_p and $(N_t+N_{^3He})/N_p$ fixed.

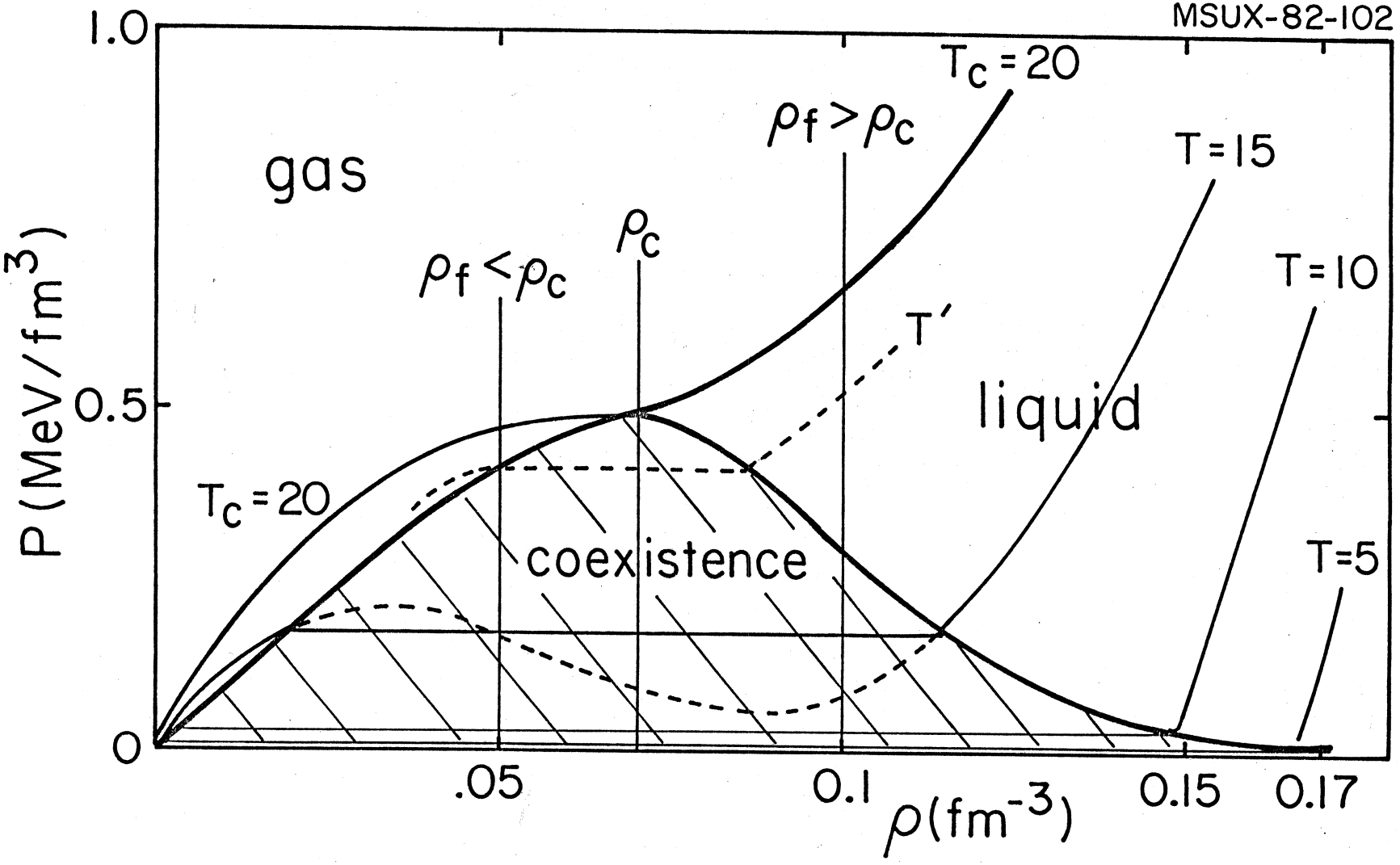
MSUX-82-102
1.0
0.5
0
P (MeV/fm^3)
$T_c = 20$
$\rho_f > \rho_c$
gas
$\rho_f < \rho_c$
ρ_c
T = 15
T = 10
T'
liquid
$T_c = 20$
coexistence
T=5
.05
0.1
0.15
0.17
ρ(fm^{-3})

MSUX-82-103

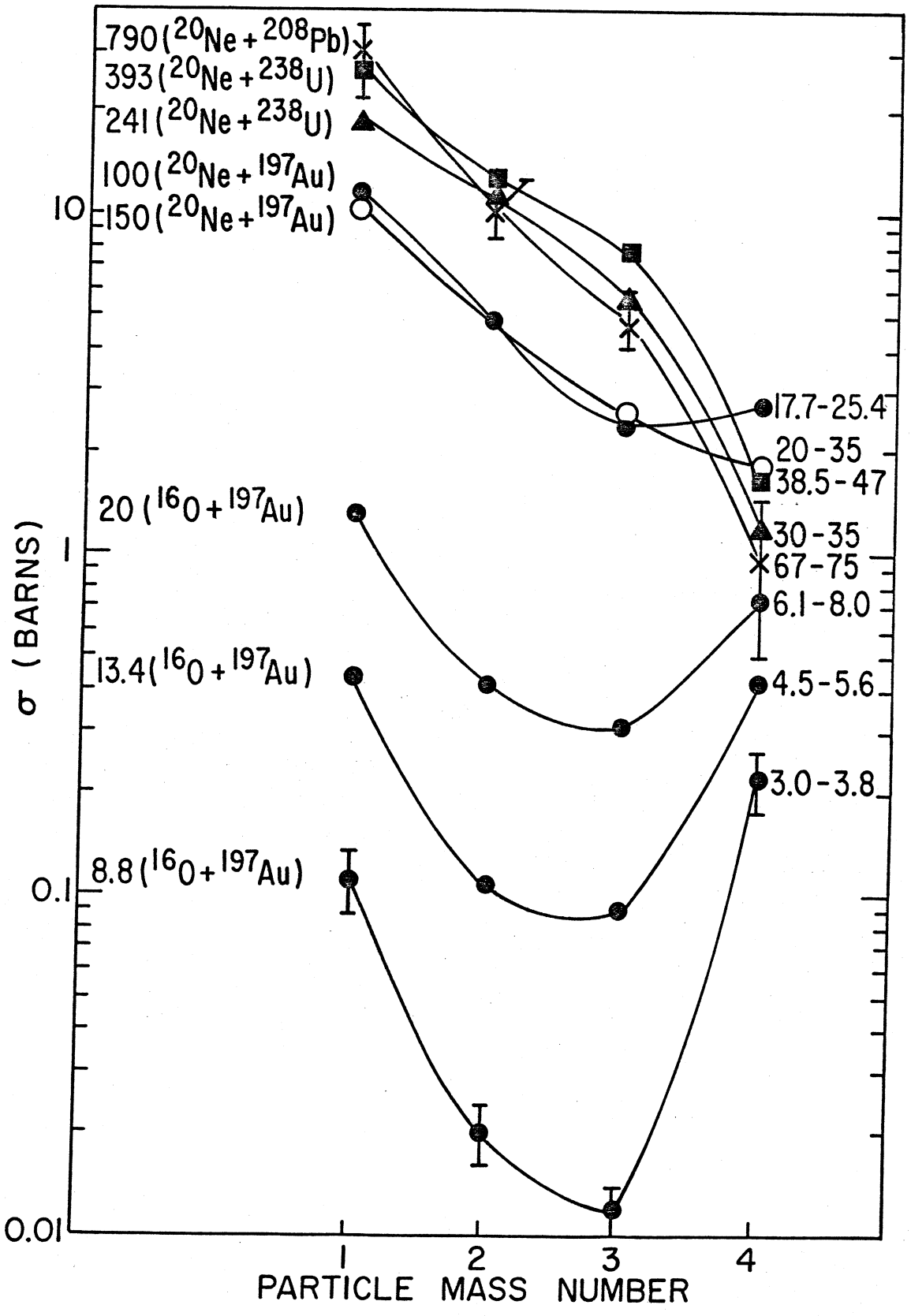
790(^{20}Ne + ^{208}Pb)
393(^{20}Ne + ^{238}U)
241(^{20}Ne + ^{238}U)
100(^{20}Ne + ^{197}Au)
150(^{20}Ne + ^{197}Au)
20(^{16}O + ^{197}Au)
13.4(^{16}O + ^{197}Au)
8.8(^{16}O + ^{197}Au)
17.7-25.4
20-35
38.5-47
30-35
67-75
6.1-8.0
4.5-5.6
3.0-3.8
10
1
0.1
0.01
σ (BARNS)
1
2
3
4
PARTICLE MASS NUMBER

MSUX-82-091

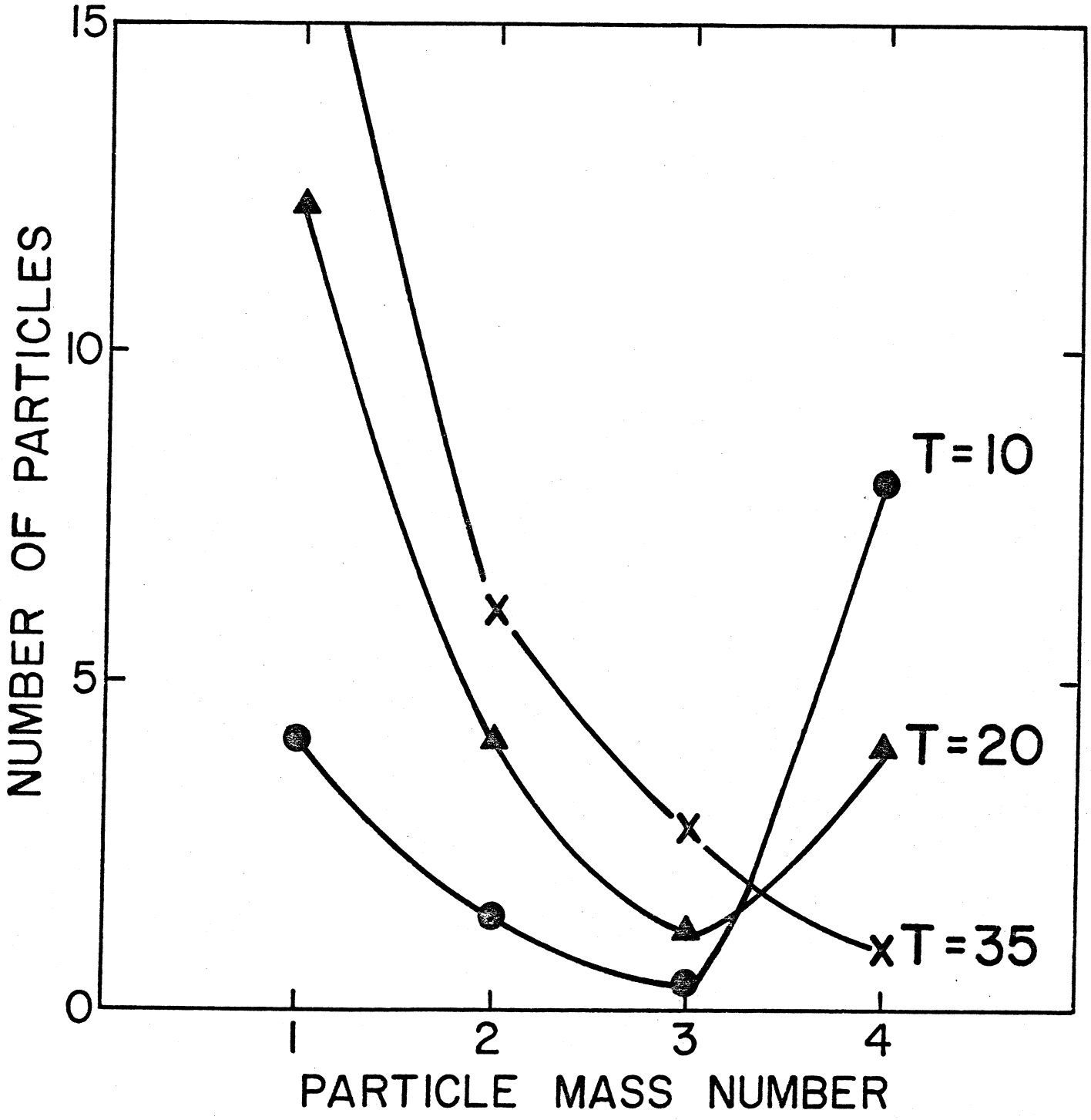
15
10
5
0
NUMBER OF PARTICLES
1
2
3
4
PARTICLE MASS NUMBER
T=10
T=20
T=35